46. More complete calculations produced an increase by factors of up to 100 in the opacity of pure iron [(62); F. J. Rogers and C. A. Iglesias, *Astrophys. J. Suppl. Ser.* **79**, 507 (1992); C. A. Iglesias, F. J. Rogers, B. G. Wilson, *Astrophys. J.* **397**, 717 (1992)] at temperatures where transitions originating in the M shell of iron dominate the absorption. This huge increase in iron opacity is enough to increase the total opacity by a factor of 2 to 3.
47. The Opacity Project [M. J. Seaton, Y. Yan, D. Mihalas, A. K. Pradhan, *Mon. Not. R. Astron. Soc.* **266**, 805 (1994); M. J. Seaton, Ed., *The Opacity Project* (Institute of Physics Publ., London, 1995), vol. **1**, and references therein] is mainly an atomic physics effort; plasma effects on occupation numbers are of secondary interest.
48. For example, pulsationally inferred masses [P. Moskalik, J. R. Buchler, A. Marom, *Astrophys. J.* **385**, 685 (1992); S. M. Kanbur and N. R. Simon, *ibid.* **420**, 880 (1994); J. Christensen-Dalsgaard and J. O. Petersen, *Astron. Astrophys.* **299**, L17 (1995)].
49. See, for example, J. Christensen-Dalsgaard, T. L. Duvall, D. O. Gough, J. W. Harvey, E. J. Rhodes Jr., *Nature* **315**, 378 (1985); S. G. Korzennik and R. K. Ulrich, *Astrophys. J.* **339**, 1144 (1989).
50. Much of the improvement arose because the enhanced opacity increased the depth of the convection zone to match more closely an earlier helioseismic determination (7). However, calculations using the new OPAL opacities and the physical-picture equation of state were able to bring the calculated value much closer to the observation [D. B. Guenther, P. Demarque, Y.-C. Kim, M. H. Pinsonneault, *Astrophys. J.* **387**, 372 (1992); J. N. Bahcall and M. H. Pinsonneault, *Rev. Mod. Phys.* **64**, 885 (1992); J. A. Guzik and A. N. Cox, *Astrophys. J.* **411**, 394 (1993)]. The inclusion of element settling in the models largely explains the residual difference.
51. Simple scaling arguments (5) show that the luminosity is inversely proportional to opacity and increases as a high power of the mean molecular weight μ. Thus, to compensate for the increase in opacity, an increase in μ, and hence in Y, is required [V. A. Baturin and S. V. Ajukov, *Astron. Rep.* **37**, 489 (1995)].
52. V. N. Tsytovich, R. Bingham, U. de Angelis, A. Forlani, M. R. Occorsio, *Astropart. Phys.*, in press.
53. Such improvement in helioseismic inversion was first noted by J. Christensen-Dalsgaard, C. R. Proffitt, and M. J. Thompson [*Astrophys. J.* **403**, L75 (1993)].
54. A. G. Kosovichev, in *The Sun and Beyond: 2e Rencontres du Vietnam*, L. M. Celnikier, Ed. (Editions Frontières, Gif sur Yvette, France, in press). For a recent review, see R. S. Raghavan, *Science* **267**, 45 (1995).
55. J. N. Bahcall and H. A. Bethe, *Phys. Rev. Lett.* **65**, 2233 (1990); J. N. Bahcall, *Phys. Lett. B* **33**, 276 (1994).
56. The helioseismic inferences constrain the solar pressure, density, and sound speed. With no further constraints, this leaves considerable freedom for the temperature and composition profile and hence for the neutrinos. Note, for example, that for a fully ionized ideal gas, $c^2 \propto T/\mu$; hence, T/μ is constrained, but T and μ separately are not [H. M. Antia and S. M. Chitre, *Astrophys. J.* **442**, 434 (1995)]. Models can be found that agree with both the helioseismic data and the ^{37}Cl neutrino detections; however, the internal opacity would have to be substantially reduced in such models.
57. T. M. Brown, *Annu. Rev. Astron. Astrophys.* **32**, 37 (1994).
58. V. Canuto and I. Mazzitelli, *Astrophys. J.* **370**, 295 (1991).
59. J. N. Bahcall and M. H. Pinsonneault, *Rev. Mod. Phys.* **67**, 781 (1995).
60. A. N. Cox, J. A. Guzik, R. B. Kidman, *Astrophys. J.* **342**, 1187 (1989).
61. G. Michaud and C. R. Proffitt, in *Inside the Stars*, A. Baglin and W. W. Weiss, Eds. (IAU Colloq. 137, ASP Conf. Ser. 40, Astronomical Society of the Pacific, San Francisco, 1993), p. 246.
62. C. A. Iglesias and F. J. Rogers, *Astrophys. J.* **371**, L73 (1991).
63. D. O. Gough and J. Toomre, *Annu. Rev. Astron. Astrophys.* **29**, 627 (1991).
64. S. Basu and H. M. Antia, *J. Astrophys. Astron.* **15**, 143 (1994). Convection was treated using the Canuto and Mazzitelli formulation (58).
65. A. G. Kosovichev, in *Proceedings of the Fourth SOHO Workshop: Helioseismology*, J. T. Hoeksema, V. Domingo, B. Fleck, B. Battrick, Eds. (ESA SP-376, European Space Research and Technology Centre, Noordwijk, Netherlands, 1995), vol. 1, p. 165.
66. C. S. Rosenthal *et al.*, *ibid.*, vol. 2, p. 459.
67. We thank R. Trampedach for assistance with the graphics. The work reported here was supported in part by the Danish National Research Foundation through the establishment of the Theoretical Astrophysics Center and in part by grant AST-9315112 from National Science Foundation (NSF). The GONG is managed by the National Solar Observatory, a division of the National Optical Astronomy Observatories, operated by Association of Universities for Research in Astronomy under a cooperative agreement with NSF. The data were acquired by instruments operated by the Big Bear Solar Observatory, High Altitude Observatory, Learmonth Solar Observatory, Udaipur Solar Observatory, Instituto de Astrofísica de Canarias, and Cerro Tololo Interamerican Observatory.

18 March 1996; accepted 10 May 1996

The Solar Acoustic Spectrum and Eigenmode Parameters

F. Hill, P. B. Stark, R. T. Stebbins, E. R. Anderson, H. M. Antia, T. M. Brown, T. L. Duvall Jr., D. A. Haber, J. W. Harvey, D. H. Hathaway, R. Howe, R. P. Hubbard, H. P. Jones, J. R. Kennedy, S. G. Korzennik, A. G. Kosovichev, J. W. Leibacher, K. G. Libbrecht, J. A. Pintar, E. J. Rhodes Jr., J. Schou, M. J. Thompson, S. Tomczyk, C. G. Toner, R. Toussaint, W. E. Williams

The Global Oscillation Network Group (GONG) project estimates the frequencies, amplitudes, and linewidths of more than 250,000 acoustic resonances of the sun from data sets lasting 36 days. The frequency resolution of a single data set is 0.321 microhertz. For frequencies averaged over the azimuthal order m, the median formal error is 0.044 microhertz, and the associated median fractional error is 1.6×10^{-5}. For a 3-year data set, the fractional error is expected to be 3×10^{-6}. The GONG m-averaged frequency measurements differ from other helioseismic data sets by 0.03 to 0.08 microhertz. The differences arise from a combination of systematic errors, random errors, and possible changes in solar structure.

Several million resonant acoustic normal modes (eigenmodes) of the sun are excited stochastically in the subsurface turbulent layer. The frequencies ν, amplitudes A, and characteristic widths Γ of such modes, as a function of radial order n, spherical harmonic degree ℓ, and azimuthal order m, form the basic data from which helioseismic inferences about the solar interior are drawn. The GONG project currently estimates these eigenspectral parameters for about 250,000 normal modes every 36 days, with the potential to estimate parameters for more than one million modes. Here we discuss solar oscillation spectra and random and systematic errors in the estimated mode parameters and compare GONG mode frequency estimates to those derived from three other experiments.

The amplitudes of solar oscillations are sufficiently small that linear oscillation theory is an excellent approximation. Nonetheless, there are numerous statistical problems in estimating the mode parameters from the surface motions of the sun as observed by the GONG instruments. These problems include estimating the geometry of the images of the solar disk, estimating the modulation transfer function (MTF) of the instrument and atmosphere, estimating systematic and stochastic components of the observational noise, optimally combining observations obtained at different sites into coherent time series, dealing with missing observations, and estimating parameters of a three-dimensional power spectrum and their errors and covariances. Because we observe only a portion of one side of the sun, some power leaks across spatial frequencies; this leakage makes it difficult to separate modes and distinguish splitting caused by the solar structure from that of artifacts of the observation and reduction process. The sun changes on time scales of 1 month, so common statistical prescriptions, based on frequency resolution and variance, for partitioning the years of data into shorter time series and combining their spectra do not apply directly; other methods are necessary. Similarly, the stochastic nature of the excitation process could be exploited to improve eigenspectral estimates, and statistical properties of the excitation process are interesting themselves. Our knowledge of the solar interior will become more precise as improved statistical techniques, tailored specifically to this problem, are developed and applied to the growing body of GONG data. The current limitation on the accuracy and precision of helioseismic estimates of solar structure from GONG data lies in the details of the data reduction.

Solar Oscillation Spectra

A typical three-dimensional solar acoustic spectrum (Fig. 1) at $\ell = 85$ contains sets of discrete ridges; each set corresponds to a different value of n. Within each set, further ridges are visible. These arise mainly from the approximate decomposition of the motion of the observable part of the sun into spherical harmonics: because spherical harmonics are not orthogonal over the observed portion of the sun (somewhat less than a hemisphere), the spectrum at a target degree ℓ_t contains power from adjacent values of ℓ. This power appears at frequencies appropriate to the degrees of the spatial leaks. If it were possible to observe the entire surface of the sun, these spatial side lobes would be substantially reduced, but contributions to the side lobes from projection effects and the horizontal component of the oscillatory velocity field would remain. GONG spectra have fewer and smaller artifacts than single-site data, which suffer spectral leakage resulting from the periodic interruption of the observations between sunset and sunrise.

The standard GONG data products—network spectra and mode parameters—are produced every 36 days to sample (but not to be synchronized with) the synodic solar rotation period of 27 to 32 days. For some purposes it is advantageous to combine data over longer time periods either coherently or incoherently. A coherent analysis concatenates several 36-day time series, preserving phase information. This combination increases the frequency resolution but does not reduce stochastic noise. Resolution is improved significantly for modes with long lifetimes (small Γ) (Fig. 2); these modes typically have low ν. GONG will produce spectra from 1-year time series for $\ell \leq 30$. Data can also be combined incoherently by averaging together power spectra from several months. This averaging reduces the stochastic noise, producing a smoother spectrum, but does not increase the frequency resolution. A combination of these approaches allows one to reduce the bias from poor frequency resolution and the variance from stochastic excitation and other sources of noise, but there is a practical upper limit to the length of time series, beyond which we incur bias from temporal changes in solar properties.

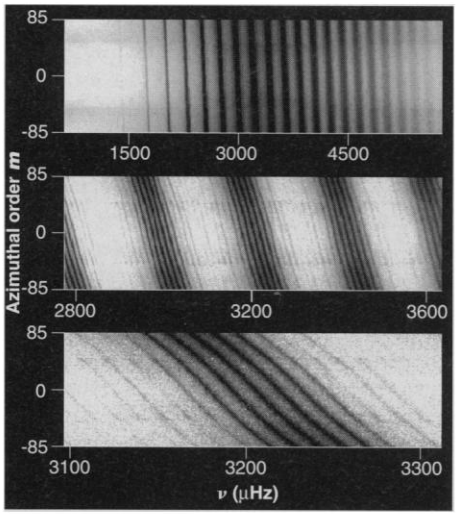

Fig. 1. An example of an m-ν spectrum for $\ell = 85$, obtained between 23 August 1995 and 18 February 1996. The spectrum is shown at three magnifications to display the spatial side lobes that result from observing only a fraction of the solar surface.

Sources of Error and Uncertainty

There are many sources of uncertainty: external (*1*), instrumental (*2*), and data processing (*3*). To evaluate errors in the GONG eigenfrequency estimates, we used band-passed root mean square (rms) power images to study the differences in velocity noise patterns at different frequencies. At high frequencies, the rms velocity is independent of azimuth and shows a small increase near the center resulting from small residual image motion convolved with the pattern of solar intensity structures (which is strongest near the center of the image) and photon counting noise (which increases toward the limb). At pressure- (p-) mode frequencies, the power has a somewhat larger increase near the center because the velocity of p modes is predominantly normal to the solar surface. At lower frequencies, the rms values are larger near the limb because supergranule flow velocities are predominantly horizontal. A formal propagation of photon and camera readout noise through the velocity calibration shows that the nonoscillatory solar background contribution is at least two orders of magnitude higher than the camera noise for most values of ℓ and ν.

Differences between estimates derived from stations simultaneously observing the sun measure uncertainties attributable to instrument and calibration effects, image rotation, estimates of the MTF, geometric corrections, and image registration. The relative power in the difference of spherical

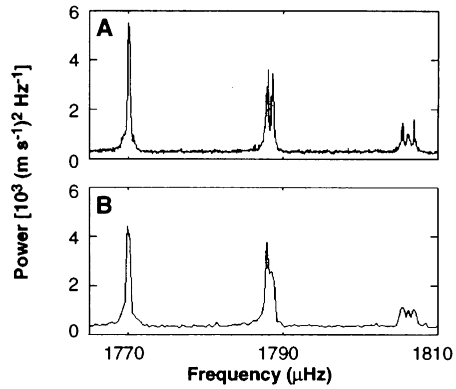

Fig. 2. Increase in frequency resolution of a frequency-shifted m-averaged spectrum resulting from the coherent concatenation of longer strings of data. (**A**) Portion of the oscillation spectrum obtained from a 180-day time series. (**B**) The same portion of the oscillation spectrum shown in (A) from a 36-day time series. The fine structure in the peaks arising from leakage with modes at different m is more clearly resolved in (A), the spectrum of the longer time series.

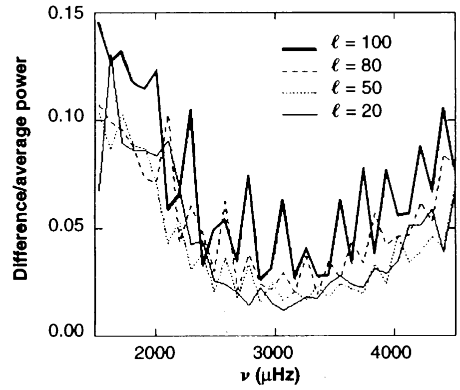

Fig. 3. Power spectrum of the difference between simultaneous observations of the sun at Teide and Udaipur, normalized by the average power at the two sites. This plot provides a measure of the errors in the power spectra arising from variations between instruments, seeing, pointing, and data processing.

F. Hill, E. R. Anderson, J. W. Harvey, R. P. Hubbard, J. R. Kennedy, J. W. Leibacher, J. A. Pintar, C. G. Toner, R. Toussaint, and W. E. Williams are with the National Solar Observatory, National Optical Astronomy Observatories (NOAO), Post Office Box 26732, Tucson, AZ 85726–6732, USA. P. B. Stark is with the Department of Statistics and Space Sciences Laboratory, University of California, Berkeley, CA 94720, USA. R. T. Stebbins and D. A. Haber are with JILA, University of Colorado, Boulder, CO 80309, USA. H. M. Antia is with the Tata Institute of Fundamental Research, Bombay, India. T. M. Brown and S. Tomczyk are with the High Altitude Observatory, National Center for Atmospheric Research, Boulder, CO 80307, USA. T. L. Duvall is with the NASA Goddard Space Flight Center, Stanford University, Center for Space Science and Astrophysics (CSSA), Stanford, CA 94305, USA. D. H. Hathaway is with the NASA Marshall Space Flight Center, Mail Code ES82, Huntsville, AL 35812, USA. R. Howe and M. J. Thompson are with the Astronomy Unit, Queen Mary and Westfield College, London E1 4NS, UK. H. P. Jones is with the NASA Goddard Space Flight Center Southwest Station, NOAO, Tucson, AZ 85726, USA. S. G. Korzennik is with the Harvard-Smithsonian Center for Astrophysics, 60 Garden Street, Cambridge, MA 02138, USA. A. G. Kosovichev and J. Schou are with Stanford University, CSSA, Stanford, CA 94305, USA. K. G. Libbrecht is with the California Institute of Technology, 264-33, Pasadena, CA 91125, USA. E. J. Rhodes is with the Department of Physics and Astronomy, University of Southern California, Los Angeles, CA 90089, USA.

harmonic time series derived from two stations observing the sun at the same time is typically low in the p-mode band (Fig. 3). Thus, the differences among instruments are small, as are those among errors in MTF estimates, geometry estimates, image registration, and restored images values. The dominant source of the residual differences is image registration—that is, the location and angular orientation of the image of the sun on the CCD (charge-coupled device), which is estimated for each image in an early stage of data reduction.

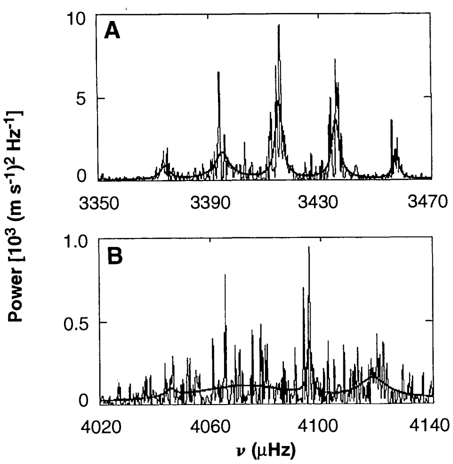

Fig. 4. Power spectra of spherical harmonic time series and the parametric functions fitted to them to estimate the frequencies, amplitudes, and linewidths of the normal modes they contain. (**A**) High-quality fit at $\ell = 50$, $m = -32$, $n = 12$; the uncertainty in the estimated mode parameters is small. (**B**) Poor fit at $\ell = 50$, $m = 0$, $n = 16$; the estimated parameters were automatically flagged as untrustworthy. Note the different power levels in these spectra.

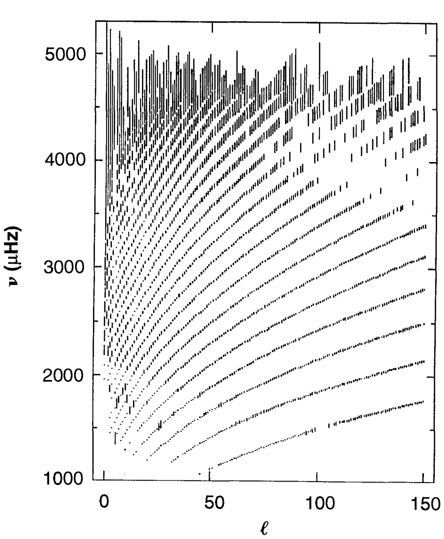

Fig. 5. Central frequencies ν averaged over m measured between 28 September 1995 and 3 November 1995. The errors bars represent the formal errors of the fitted frequencies multiplied by a factor of 200.

A major source of uncertainty is in estimating mode parameters from the spectra. Mode parameters ν, A, and Γ are estimated from the spectrum by maximizing an approximation to the likelihood function, on the assumption that the spectrum is a superposition of Lorentzian peaks (4). The combination of stochastic variability, spectral leakage resulting from incomplete spatial coverage, and variable signal-to-noise ratio (SNR) as a function of ℓ and ν can make it difficult to estimate mode parameters accurately (Fig. 4). However, spectra from the network have small temporal side lobes, thus fewer peaks to fit, and smaller systematic errors compared with single-site data.

Currently, the GONG project estimates parameters of modes with $\nu \approx 1.5$ to 5 mHz, ℓ between 0 and 150, and all relevant values of m. This data set represents only about 25% of the modes that contribute to the observed spectra, which include $0 \leq \ell \leq 250$ and $0 \leq \nu \leq 8.33$ mHz. The restricted region includes all modes that live long enough to be global (producing discrete peaks in the power spectrum), where spatial aliasing is weak and the SNR is high. Above $\ell \approx 180$, modes are local short-lived oscillations with broader linewidths, and the frequency spacing between oscillations with adjacent ℓ decreases; as a result, the peaks blend into ridges.

While measurements of $\nu(\ell,m,n)$ are used to infer the solar angular velocity and asphericity as a function of depth and latitude (5, 6), it is also useful to average ν over m (Fig. 5). Averaging reduces the noise in the estimate of ν, and the averaged frequencies can be used to estimate the radial stratification of the density, the speed of sound, and the chemical composition in the solar interior with higher accuracy (6). However, the effect of rotation (which gives rise to the curvature of the ridges in Fig. 1) must be removed before averaging, otherwise the m-averaged mode widths will be overestimated. The effect of rotation is removed by frequency shifting the spectrum for each m (5).

Currently, the reported errors in the mode parameter estimates are formal and reflect primarily the sensitivity of the parameter-fitting algorithm in the neighborhood of the estimate. Over a 36-day time series of observations, the median formal error in the m-averaged frequencies is about 44 nHz (about 14% of one resolution element in ν), and the median fractional error is 1.6×10^{-5}. These errors should decrease as the frequency resolution improves. For 1-year time series, the mean formal error is expected to be about 14 nHz (a fractional error of 5×10^{-6}); over the first 3 years of the project, a mean formal error of 8 nHz (fractional error of 3×10^{-6}) is expected.

Although the peak-fitting algorithm assumes that every peak has a specific symmetric shape and background, both are asymmetric in some regions of the spectrum (7). Neglecting these effects probably introduces a small systematic error in the estimated frequencies. We explored the effect of the starting values on the peak-fitting algorithm by starting the algorithm from randomly generated values about the reference frequencies. The resulting frequency estimates changed on the average by less than 5% of their nominal uncertainties for modes with frequencies in the range 1.8 to 3.3 mHz.

Comparison with Other Data Sets

A number of earlier experiments have measured parameters of the modes observed by GONG (8). We examined the differences between m-averaged frequencies obtained by GONG and three other experiments (9), as well as differences between two months of GONG data (Fig. 6). Mode frequencies es-

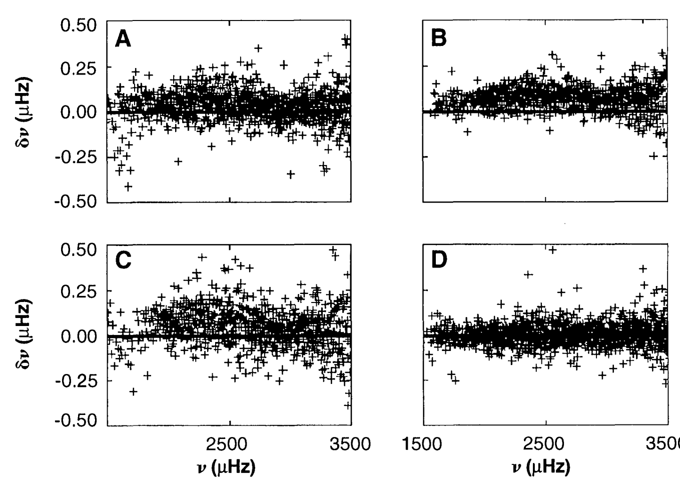

Fig. 6. Comparisons of the m-averaged frequencies obtained by GONG between 23 August 1995 and 27 September 1995 with frequencies from other experiments. (**A**) Comparison with estimates from Big Bear Solar Observatory data recorded in 1986. (**B**) Comparison with estimates from LOWL data collected between 26 February 1994 and 25 February 1995. (**C**) Comparison with estimates from coeval Mount Wilson data obtained between 23 August 1995 and 27 September 1995. (**D**) Comparison with estimates from GONG data obtained between 28 September 1995 and 3 November 1995.

timated from Big Bear Solar Observatory data obtained at a time of comparable solar activity differ from GONG estimates by a mean (±SD) of 29 ± 86 nHz. Mode frequency estimates from the High-Altitude Observatory (HAO) Low-ℓ Instrument (LOWL) data, obtained about 1 year before the GONG data, differ from GONG estimates by 74 ± 81 nHz. Data from Mount Wilson and GONG are virtually coeval; their mean difference is 48 ± 110 nHz. Although the mean differences are smaller than the standard deviations of the differences, suggesting that the deviations are consistent with zero, the GONG frequency estimates are systematically lower than those of the other three experiments (Fig. 6).

The differences between the GONG results and the others represent a combination of systematic errors, random errors, possible changes in solar structure and dynamics, and variations in solar activity. Evolving solar magnetic activity can produce temporal variations in mode frequencies because the frequencies depend on the level of surface activity (*10*). These effects also contribute to changes in the GONG frequency estimates from month to month.

The effects of solar changes are substantially eliminated in the Mount Wilson–GONG comparison because the data were collected simultaneously. Their difference is probably dominated by a combination of unknown systematic errors in both data sets. There is also indication that the difference depends on ν in both the Mount Wilson–GONG and the LOWL-GONG comparisons. Although the actual causes of the frequency differences remain uncertain, GONG's higher duty cycle, compared with the other experiments, reduces temporal-gap artifacts and improves the SNR. The MTF correction could contribute to the differences; it is applied in the GONG analysis but not in any of the others. Other details of the data analysis, such as the peak-fitting algorithm and the m-averaging, also play a role.

Comparing spectral estimates from 2 months of GONG data estimates the reproducibility of m-averaged frequencies obtained by GONG. The mean difference is 3.7 ± 66 nHz. The standard deviation is about a factor of $\sqrt{2}$ larger than the median of the error estimated by the fitting procedure for 1 month (44 nHz). Systematic errors should be essentially identical in both data sets, and the contribution of activity should be small and similar for both months, because solar activity is near minimum.

The identification and estimation of systematic errors is one of the major statistical challenges in helioseismology. Systematic errors in the estimated frequencies result in comparable errors in the inference of solar structure and dynamics. The Solar and Heliospheric Observatory–Solar Oscillations Investigation (SOHO-SOI) experiment was launched in December 1995 (*11*) and will provide high-ℓ observations complementary to those obtained by GONG. Comparison of SOI and GONG data will provide estimates of the systematic errors in both data sets.

REFERENCES AND NOTES

1. External sources include other solar velocity fields, attenuation of the oscillations in active regions, terrestrial atmospheric transparency variations (including birds and other opaque objects in the field of view), and seeing and atmospheric scattering.
2. Instrumental sources include prefilter nonlinearity and drift, image rotator encoder errors, spatial aliasing, spurious modulation, camera nonlinearity and zero-level variations, nonlinearity of velocity and intensity during integration, and image cache differences.
3. Data processing sources include calibration; image geometry determination; remapping of residuals from refraction, line-of-sight velocity projection, and pixellation; ephemeris errors; spherical harmonic approximation to true eigenfunctions; merging errors from MTF approximation and velocity scale factors; gap-filling; and peak fitting (leakage, parametric model, and algorithm).
4. E. Anderson, T. Duvall, S. Jefferies, *Astrophys. J.* **364**, 699 (1990). For other approaches to estimating mode parameters, see S. Korzennik, thesis, University of California at Los Angeles (1990); J. Schou, thesis, University of Aarhus (1992); J. Patrón, thesis, Universidad de La Laguna (1994); and (*12*).
5. M. J. Thompson *et al.*, *Science* **272**, 1300 (1996), and references therein.
6. D. O. Gough *et al.*, *ibid*, p. 1296, and references therein.
7. Observations indicate substantial deviations of the line profile from a symmetrical Lorentzian shape. The line asymmetry is particularly pronounced for low- and high-frequency p modes. The degree of the asymmetry depends on the location of the excitation sources of oscillations relative to the mode resonant cavity [T. L. Duvall Jr. *et al.*, *Astrophys. J.* **410**, 829 (1993); M. Gabriel, *Astron. Astrophys.* **299**, 245 (1995)].
8. Observational helioseismology has an extensive literature. A short list of representative papers from other observational efforts in the last decade is given. Big Bear Solar Observatory: (*13*); National Solar Observatory (NSO)–South Pole: T. L. Duvall Jr. *et al.*, *Astrophys. J.* **324**, 1158 (1988); Mount Wilson–Univ. of Southern California (USC): (*14*); Birmingham Solar Oscillation Network (BiSON): Y. Elsworth *et al.*, *Astrophys. J.* **434**, 801 (1994); Université de Nice International Research on the Interior of the SUN (IRIS) Network: S. Loudagh *et al.*, *Astron. Astrophys.* **275**, L25 (1993); HAO Fourier Tachometer: K. T. Bachmann, J. Schou, T. Brown, *Astrophys. J.* **412**, 870 (1993); NSO–High-ℓ Helioseismometer: (*12*); Univ. of Hawaii Photometric Oscillations Imager: R. S. Ronan and B. J. LaBonte, *Sol. Phys.* **149**, 1 (1994); Taiwanese Oscillations Network (TON): D.-Y. Chou *et al.*, *ibid.* **160**, 237 (1995); LOWL: (*15*).
9. Big Bear Solar Observatory: (*13*); LOWL: (*15*); Mount Wilson–USC: (*14*).
10. The frequencies of the p modes increase as the surface activity increases. The frequency shift depends on ν and is about 0.4 μHz for $\nu \approx 3$ mHz. The shift is thought to result from a combination of magnetic and temperature effects. Observational papers on the subject include M. F. Woodard and R. W. Noyes, *Nature* **318**, 449 (1985); E. J. Rhodes Jr. *et al.*, *Astrophys. J.* **326**, 479 (1988); K. G. Libbrecht and M. F. Woodard, *Nature* **345**, 779 (1990); Y. Elsworth *et al.*, *ibid.*, p. 322; M. Anguera Gubau *et al.*, *Astron. Astrophys.* **255**, 363 (1992); and K. T. Bachmann and T. M. Brown, *Astrophys. J.* **411**, L45 (1993). There is also evidence for a solar cycle variation in Γ [S. M. Jefferies *et al.*, *Astrophys. J.* **377**, 330 (1991)] and in A [Y. Elsworth *et al.*, *Mon. Not. R. Astron. Soc.* **265**, 888 (1993)].
11. P. H. Scherrer *et al.*, *Sol. Phys.* **162**, 129 (1995).
12. K. T. Bachmann, T. L. Duvall Jr., J. W. Harvey, F. Hill, *Astrophys. J.* **443**, 837 (1995).
13. K. G. Libbrecht, M. F. Woodard, J. M. Kaufman, *Astrophys. J. Suppl. Ser.* **74**, 1129 (1990).
14. E. J. Rhodes Jr., A. Cacciani, S. G. Korzennik, *Adv. Space Res.* **11**, 17 (1991).
15. S. Tomczyk *et al.*, *Sol. Phys.* **159**, 1 (1995).

16. The GONG project is managed by NSO, a division of the NOAO, which is operated by the Association of Universities for Research in Astronomy under a cooperative agreement with NSF. The data were acquired by instruments operated by Big Bear Solar Observatory, HAO, Learmouth Solar Observatory, Udaipur Solar Observatory, Instituto de Astrofísica de Canarias, and Cerro Tololo Interamerican Observatory.

18 March 1996; accepted 7 May 1996